https://doi.org/10.5194/egusphere-2024-1961
Preprint. Discussion started: 25 July 2024

Impact of introducing electric vehicles on ground-level O_3 and $PM_{2.5}$ in the Greater Tokyo Area: Yearly trends and the importance of changes in the Urban Heat Island effect

Hiroo Hata[1], Norifumi Mizushima[2], Tomohiko Ihara[3]

[1] Research Institute of Science for Safety and Sustainability, National Institute of Advanced Industrial Science and Technology (AIST), 16-1 Onogawa, Tsukuba, Ibaraki 305-8569, Japan
[2] Research Institute for Energy Conservation, National Institute of Advanced Industrial Science and Technology (AIST), 1-2-1 Namiki, Tsukuba, Ibaraki 305-8564, Japan
[3] Department of Environment Systems, Graduate School of Frontier Sciences, The University of Tokyo, 5-1-5 Kashiwanoha, Kashiwa, Chiba 277-8563, Japan

Correspondence to: Hiroo Hata (hata-hiroo@aist.go.jp)

Abstract. Battery electric vehicles (BEVs) are considered a solution for global warming and air pollution, and several countries have announced a shift to BEVs in the 2030s. This study is an evaluation of changes in the urban heat island (UHI) effect in the Greater Tokyo Area (GTA) of Japan as a result of introducing BEVs using numerical weather prediction. The results indicated that the substitution of internal combustion vehicles with BEVs led to a maximum decrease of 0.2 °C in the local temperature for the metropolitan GTA. Estimation of the effects of introducing BEVs on tropospheric ozone (O_3) and fine particulate matter ($PM_{2.5}$) using a regional chemical transport model indicated that mitigating against the UHI effect led to a decline in the ground-level O_3 formation due to decreased atmospheric chemical reactions and lower biogenic volatile organic compounds (BVOC). The decrease in vehicular exhaust emissions and increase in power plant emissions were nonlinear, and the total change in O_3 depends on season and location. The temperature decrease that resulted from the mitigation of UHI resulted in enhanced particle coagulation, with an increase in ground-level $PM_{2.5}$ formation in several regions. Furthermore, a decrease in the BVOC emissions also resulted in increased $PM_{2.5}$ owing to enhancement of the OH + SO_2 reaction. The total prevented annual premature deaths of 175 and 77 that resulted from the changes in O_3 and $PM_{2.5}$, respectively, indicate the positive effects of BEV introduction on air quality management in the GTA, and may be applicable to other megacities worldwide.

1 Introduction

Climate change has significantly impacted global temperatures, inducing natural hazards and health problems (Heidari and Pearce, 2016; Dubash et al., 2018; Iacobuta et al., 2018; Fox et al., 2019). In response, worldwide organizations are attempting to restrict greenhouse gas (GHG) emissions, with the target of minimizing the temperature increase from the era of the industrial revolution to only 1.5 °C or 2.0 °C by 2100 (Fawzy et al., 2020; Schreyer et al., 2020; Strapason et al., 2020), and

https://doi.org/10.5194/egusphere-2024-1961
Preprint. Discussion started: 25 July 2024

governments, especially in developed countries, have set future scenarios with the goal of achieving net zero-carbon societies. The transport sector is known to be a large GHG emission source; thus, the introduction of battery electric vehicles (BEVs) is considered one solution by which emissions can be minimized (Moro and Lonza, 2018; Shen et al., 2019; Andersson and Börjesson, 2021). The introduction of BEVs is also expected to decrease primary air pollutant emissions from engine exhaust and the evaporation of gasoline (Soet et al., 2014; Ferero et al., 2016; Requia et al., 2018). The nitrogen oxides (NO_X) and volatile organic compounds (VOCs) that are emitted by vehicles are precursors of tropospheric ozone (O_3) and fine particulate matter ($PM_{2.5}$), which are harmful to animals, including humans (Finlayson-Pitts and Pitts Jr., 1993; Sillman, 1999; Volkamer et al., 2006; Holmes, 2007). The introduction of BEVs is thus expected to decrease these precursors. Aside from the direct exhaust emission issue, Muratori suggested that there would be an increased power demand due to BEV battery charging (Muratori, 2018), which suggests an increase in emissions of primary air pollutants from power plants attributable to the introduction of BEVs. Furthermore, the anthropogenic heat (AH) from vehicles is expected to decrease by the introduction of BEVs because of the mitigation of engine exhaust emissions. According to the review article of Ulpiani, the mechanisms of the impact of the UHI effect on air pollutants are associated with: (1) the change of the kinetics of O_3 (and $PM_{2.5}$) formation, (2) the change of air mixing ratio arising from the change of ambient temperature, and (3) the change of biogenic VOC (BVOC) emissions (Ulpiani, 2021), which are all correlated with each other. Therefore, the detailed information concerning how the introduction of BEVs is likely to contribute to atmospheric pollution is particularly important in determining governmental strategies for the future.

The Greater Tokyo Area (GTA) of Japan is one of the largest regions in the world in terms of economy, population and human activities, industry, etc., and the air pollution caused by road traffic in the area remains a major concern. Previously, Hata and Tonokura conducted chemical transport modeling in the GTA to evaluate how ground-level O_3 concentrations change in response to the introduction of zero-emission vehicles (Hata and Tonokura, 2019). The study revealed ground-level O_3 increases in urban areas that were due to VOC-limited atmospheric conditions and the NO-titration effect (Santiago et al., 2022), and concluded that the health risk associated with increased O_3 surpasses that of influenza and heatstroke. which was not considered in the study conducted by Hata and Tonokura. An evaluation of the impact of nighttime BEV battery charging on ground-level O_3 by Kayaba and Kajino during the summer season in the GTA implied a non-negligible impact on the O_3 concentration (Kayaba and Kajino, 2023). However, despite the impactful findings surrounding the introduction of BEVs on the air quality in the GTA, the study targeted only O_3 as a secondary air pollutant and the evaluation of $PM_{2.5}$ was neglected, although the potential health risk of $PM_{2.5}$ is expected to be equal to or higher than O_3 (Poppe III et al., 2002; WHO Regional Office for Europe, Copenhagen, 2008). Some studies have also reported positive effects from introducing BEVs on local O_3 and $PM_{2.5}$, based on the results of chemical transport modelling (Li et al., 2016; Pan et al., 2019; Lin et al., 2020).

Despite these findings, the effects of the change of AH, which finally causes change of the urban heat island (UHI) effect, attributable to the introduction of BEVs to ground-level O_3 and $PM_{2.5}$ were never considered. Xie et al. conducted a model calculation to evaluate the effect of AH on ground-level O_3 in southern China, with results showing a high impact on O_3 formation, corresponding to a 2.5 ppb increase (Xie et al., 2016), and other studies have also indicated a positive correlation

https://doi.org/10.5194/egusphere-2024-1961
Preprint. Discussion started: 25 July 2024

between O_3 and the UHI effect (Stathopoulou et al., 2008; Wang et al., 2018; Ulpiani, 2021). The introduction of BEVs is expected to decrease the local UHI effect by reducing AH (Li et al., 2015). Thus, a more accurate evaluation of the impact of introducing BEVs on the local air quality that considers changes in the UHI is required to assist in policymaking.

The purpose of this study was therefore to clarify the yearly impact of the introduction of BEVs on ground-level O_3 and $PM_{2.5}$ while also examining the effect of the UHI mitigation on O_3 and $PM_{2.5}$ production in the GTA. The impact of changes to the UHI that result from the introduction of BEVs on the formation of the two atmospheric pollutants was evaluated using a chemical transport model coupled with numerical weather prediction. A detailed analysis of the changes in ground-level O_3 and $PM_{2.5}$ was conducted within the scope of atmospheric chemistry. Finally, the change in premature mortality in the GTA due to the introduction of BEVs was estimated as a representative health risk. To the best of our knowledge, this is the first study to consider the UHI effect that is caused by the shift to BEVs for road transportation on O_3 and $PM_{2.5}$ using chemical transport model. Although the target region of this study is the GTA in Japan, the results are expected to be referenced by other megacities, thus contributing to policymaking worldwide.

2 Methodology

2.1 Scenarios for the replacement of internal combustion vehicles with battery electric vehicles

The target of this study is the replacement of internal combustion vehicles (ICVs) with BEVs. Nine categories of vehicles were applied in the emissions inventory of this study: light and normal passenger cars (PV), buses, light and small tracks (TV), heavy-duty vehicles (HV), motorcycles, and vehicles used for specific purposes (Shibata and Morikawa, 2021). The worldwide strategy to mitigate GHG reduction focuses on the complete substitution of ICVs with BEVs over the period 2030 to 2035 (Mulrow and Grubert, 2023), with net zero emissions from all vehicles by 2050. Owing to technological issues related to the capacity of batteries used in BEVs, it remains unclear whether HVs can be completely electrified (Forrest et al., 2020), and several plans have suggested the introduction of renewable fuels instead of electrification for these vehicles (Hosseinzadeh-Bandbafha et al., 2021). For these reasons, BEV replacement concentrated only on PVs and TVs in this study. The electrification strategy for motorcycles and specific purpose vehicles is not clear, and the impact of these vehicles on air pollution is expected to be less than that of other vehicles in Japan; thus, the electrification for these vehicles also was not included in the study.

2.2 Numerical Weather Predictions

2.2.1 General information

A Weather Research and Forecasting Model (WRF v4.3.3) was used to obtain meteorological conditions (Skamarock et al., 2024) from Dec. 1, 2016 to Dec. 31, 2017. The first month was treated as the spin-off period and the whole of 2017 as the analysis period. Fig. 1 shows the included domains: East Asia (D1: 45 × 45 km), Japan (D2: 15 × 15 km), and the GTA (D3:

https://doi.org/10.5194/egusphere-2024-1961
Preprint. Discussion started: 25 July 2024

95 5 × 5 km). Objective analysis data describing the boundary conditions were obtained at a resolution of 1° × 1° from the Final Atmospheric Research provided by the National Center for Atmospheric Research (NCAR: National Center for Atmospheric Research archives, 2024). The boundary conditions of sea surface temperature for 0.082° × 0.082° were obtained from the National Oceanic and Atmospheric Administration (NOAA) (Environmental Modeling Center Archives, 2024). The modelled results were validated by comparison with observation data from the Japan Meteorological Agency (Japan Meteorological
100 Agency archives, 2024). Two sites, the metropolitan areas of Tokyo and Gunma, for which further details are listed in Table S1 of the supporting information (SI), were selected to represent urban and suburban/rural areas, respectively. A simple single-layer Urban Canopy Model (UCM: Kusaka et al., 2021) was combined with the WRF calculations so that the UHI effect before and after the introduction of BEVs could be considered. UCM parameters obtained from a previous study (Hara et al., 2010) were used to determine the urban canopy parameters for the GTA. Further details of the simulation setup for the WRF are
105 listed in Table S2 of the SI.

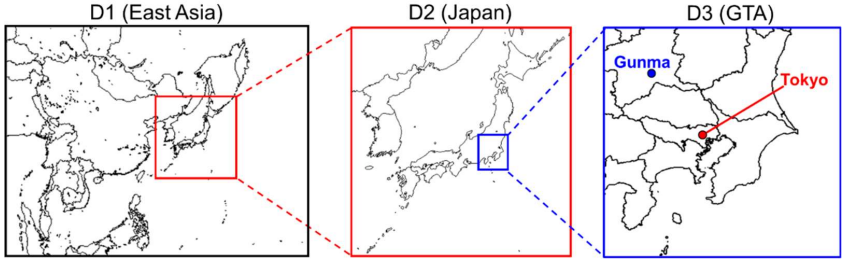

Figure 1: Domains used for numerical weather prediction and chemical transport model. Prefectural areas of Tokyo and Gunma are in domain D3.

2.2.2 Consideration of UHI effects after the introduction of BEVs

110 Several studies have suggested that UHIs are one of the results of AH from transportation (Rosenfeld et al., 1998; Nuruzzaman, 2015; Rizvi et al., 2023), and that the introduction of BEVs is expected to eradicate this issue. The changes in the total energy efficiency of BEVs as compared to ICVs affects the AH as well as vehicular exhaust emissions, leading to local changes in the UHI. The process used to evaluate AH following the introduction of BEVs is described in Appendix A. Briefly, two categories of passenger cars and one small truck listed were treated as model vehicles in this study (Tables A1 and A2), and
115 using the fuel consumption for ICVs and electric consumption for BEVs obtained using catalogue data from the manufacturers, the differences in the energy efficiencies of ICV and BEV were calculated. Statistical data concerning the number of vehicles (Database from Automobile Inspection & Registration Information Association, 2024), average mileage per year (Ministry of Land, Infrastructure, Transport, and Tourism, 2024), and the heat enthalpy of gasoline and light fuel (Agency for Natural Resources and Energy, 2024) were then applied and the total AH produced by ICVs and BEVs were calculated. Data describing
120 stationery and transportation sources in Tokyo in 2010 (Ministry of the Environment, 2024) were used to calculate the AH

https://doi.org/10.5194/egusphere-2024-1961
Preprint. Discussion started: 25 July 2024

from these sources. The results showed a reduction ratio of 0.813, or 18.7 %, for AH in the GTA in association with the introduction of BEVs.

2.3 Chemical transport modelling

2.3.1 Modelling description

A community multiscale air quality modeling system (CMAQ v5.3.3: Murphy et al., 2021) was used to calculate the air quality in Japan. Domain D3 was targeted for analysis and the year 2017 was examined, as described in Fig. 1. The period Jan. 1 to Mar. 31 was treated as winter, Apr. 1 to June 30 as spring, Jul. 1 to Sep. 30 as summer, and Oct. 1 to Dec. 31 as autumn. The meteorological inputs obtained from the results of the WRF calculations described in Sect. 2.2 were applied to the CMAQ calculation. SAPRC-07 was used to describe the gas-phase chemical mechanism (Carter, 2010), and the AERO6 module with ACM liquid chemistry as the aerosol chemical mechanism (Binkowski and Roselle, 2003). The emission inventories were provided by Chatani et al. (Chatani et al., 2018). Chemical transport modelling was validated by comparing the two observation sites listed in Table S1. The primary emissions, evaporative VOC emissions, and refueling processes associated with the use of ICVs were expected to decrease under the introduction of BEVs; however, charging batteries increases the requirement for power from plants, increasing the emissions from this source.

2.3.2 Emission changes resulting from the substitution of ICVs with BEVs

Three categories of vehicular emissions affect the environment: tailpipe engine exhaust emissions (both hot- and cold-start emissions), evaporative emissions from gasoline fleets (hot soak, diurnal breathing, and running losses), and particulate dust from tires (break, tire, and hoisting dust) (Shibata and Morikawa, 2021). Stationary sources such as VOC emissions during refueling (Yamada et al., 2018) and power plants that supply energy for battery charging (Casals et al., 2016; Kayaba and Kajino, 2023a) also require consideration. In the BEV introduction scenario, all exhaust, evaporative, and refueling emissions from the targeted vehicles were set to zero. The change in the emissions of particulate dust was not considered in this study, although a previous study suggested that brake dust increases after the introduction of BEVs owing to the weight of the battery (Kayaba and Kajino, 2023b). The increase in primary emissions from power plants that is due to charging BEVs was estimated using the value of the charging voltage of specific electric vehicles, as described in Sect. A.3 of Appendix A. The results suggested a 33.8 % increase in the amount of air pollutants from powerplants for the GTA.

2.3.3 Scenarios for the chemical transport model

Details of the two major scenarios investigated in this study: BASE, a basic scenario without the introduction of BEVs, and ALL, an BEV-introduction scenario, are listed in Table 1. The ALL scenario considers the effects of introducing BEVs and includes the emission reductions from engine exhaust and evaporative VOCs, emission increases from power plants as a result of battery charging, and UHI changes. Four sensitivity scenarios: the introduction of BEVs (S_{EV}), the increase in emissions

https://doi.org/10.5194/egusphere-2024-1961
Preprint. Discussion started: 25 July 2024

from power plants (S_{PP}), the change in ambient temperature (S_{UHI}), and the change in BVOC emissions resulting from changes to the UHI (S_{BVOC}) were also generated to evaluate the contributions of emission reduction on the formation of ground-level O_3 and $PM_{2.5}$ in GTA. Note that S_{UHI} only considers the effects of temperature change, and that the change in BVOC emissions due to such temperature changes was not included. The BASE scenario was calculated with D1, D2, and D3, while all other scenarios were calculated only for the D3 domain using the initial and boundary conditions obtained from the BASE scenario. Changes in the annual mean primary NO_X, anthropogenic VOCs (AVOC), particulate matter (PM), ammonia (NH_3), sulfur dioxide (SO_2), and BVOC emissions can be seen in Figs. S1 to S4 of the SI.

Table 2: Six scenarios calculated using the chemical transport model.

Scenario	Definition
BASE	Base scenario for 2017.
ALL	Includes total effects of substituting ICVs with BEVs.
S_{EV}	Sensitivity scenario clarifying the effect of reducing engine exhaust and evaporative emissions.
S_{PP}	Sensitivity scenario clarifying the effect of increasing power plant emissions.
S_{UHI}	Sensitivity scenario clarifying the effect of changes in the temperature as a result of AH reduction.
S_{BVOC}	Sensitivity scenario clarifying the effect of changes in the BVOCs emissions caused by the change in temperature.

3 Results

3.1 Validation of modelled temperature, O_3, and $PM_{2.5}$ with the observed results

Figure 2 shows the correlation between the observed and calculated results for the hourly ground temperature for winter, spring, summer, and autumn in Tokyo in 2017. The correlations are exhibited using four statistical factors: correlation factor (R), root mean square error (RMSE), normalized mean bias (NMB), and normalized mean error (NME). Overall, the model was found to replicate the observed results well in all seasons, with $R = 0.979$ for Tokyo and $R = 0.966$ for Gunma. Underestimations that are associated with low temperatures and overestimations that correlate with hot temperatures are within the range validated in previous studies examining the same region (Hata et al., 2020).

https://doi.org/10.5194/egusphere-2024-1961
Preprint. Discussion started: 25 July 2024

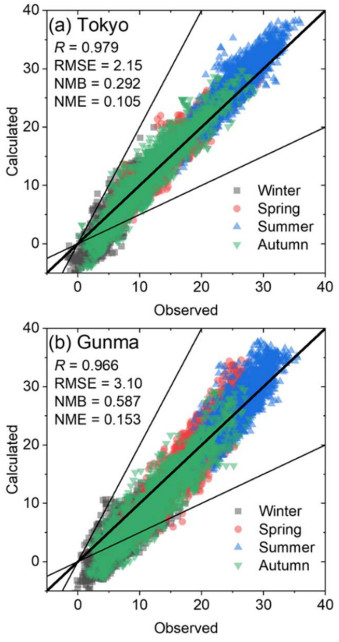

Figure 2: Comparison of observed and calculated hourly-ground temperatures for four seasons in (a) Tokyo and (b) Gunma.

Figure 3 shows the correlation between the observed and calculated (BASE) results and the 8-h daily maximum average (MDA8) O_3 concentrations. As seen in Fig. 3(a), the modeled O_3 replicated the observed results well, with most plots within a factor of two. However, Fig. 3(b) suggests less correlation for the modeled O_3 with the observed results for Gunma. Emery et al. proposed indicators that can be used to validate O_3 and $PM_{2.5}$ for chemical transport modeling (Emery et al., 2017). According to these indicators, the modeling performance for MDA8-O_3 should be $R > 0.75$, NMB $< \pm 0.05$, and NME < 0.15 while the criteria value should be $R > 0.50$, NMB $< \pm 0.15$, and NME < 0.25. Tokyo fully meets these criteria and is close to the described goals. However, Gunma did not meet the criteria for all indicators. This may be because Gunma is located in the countryside, where less primary air pollutant emissions are generated than in highly polluted areas such as Tokyo, and sources of O_3 formation in Gunma are BVOCs, transportation from other regions, and some local anthropogenic emissions, rendering it difficult to predict O_3 by CTM. Nevertheless, 70 % of the calculated results were within a factor of 2 and are thus considered acceptable for analysis.

https://doi.org/10.5194/egusphere-2024-1961
Preprint. Discussion started: 25 July 2024

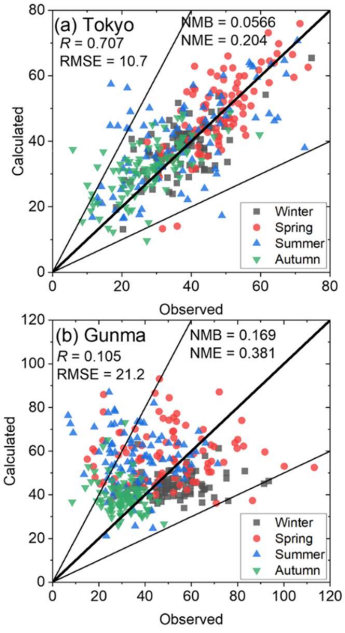

Figure 3: Comparison of observed and calculated MDA8 O_3 concentrations for four seasons in (a) Tokyo and (b) Gunma.

Figure 4 shows the correlation between the observed and calculated (BASE) results and the 24-h daily average (DA24) $PM_{2.5}$ concentrations. Emery et al. proposed that indicators to model DA24 $PM_{2.5}$ should be $R > 0.70$, NMB < ±0.10, and NME < 0.35 in terms of performance, while criteria should be $R > 0.40$, NMB < ±0.30, and NME < 0.50 (Emery et al., 2017). According to Fig. 4(a), the modeled results meet all the criteria, and some R and NME values are close to the goal. However, Fig. 4(b) shows that NMB overshoots the criteria, while R and NME meet the criteria. As mentioned above, Gunma is suburban to rural, which may explain the lower accuracy of the modeled results as compared to those obtained in urban areas. Analysis therefore considers the fact that relatively less accuracy was obtained for modeled O_3 and $PM_{2.5}$ in the Gunma region.

https://doi.org/10.5194/egusphere-2024-1961
Preprint. Discussion started: 25 July 2024

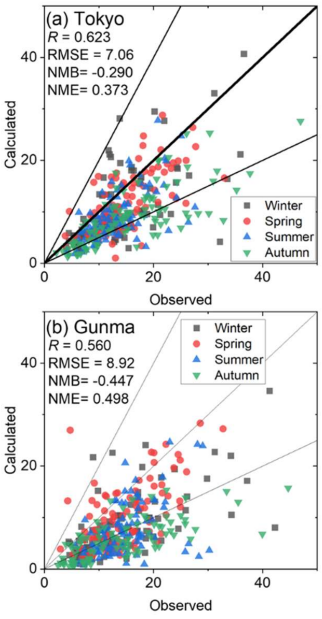

Figure 4: Comparison of observed and calculated 24-h averaged $PM_{2.5}$ concentrations for four seasons in (a) Tokyo and (b) Gunma.

3.2 UHI effect in the GTA

Figure 5 shows the average difference in the ground surface temperature (ΔT) between the BASE and ALL cases over four seasons as calculated using the WRF. The seasonal ΔT distributions are described in Fig. S5 of the SI. According to Fig. 5(a), a decrease in the average ΔT in the calculated domain is due to the decrease in AH that resulted from the introduction of BEV. According to Fig. S5, this decrease in ΔT is high in winter and autumn, and low in summer, and is distributed from the center of Tokyo, where high AH is expected as a result of condensed anthropogenic activity. The seasonal changes in ΔT for Tokyo and Gunma are extracted in Fig. 5(b), which shows a range of 0.1 °C to 0.2 °C for ΔT, with relatively high error bars, particularly for spring and summer. This is likely because of the high planetary boundary layer (PBL) that forms in the warmer seasons, which enhances thermal convection and leads to the large discrepancies observed in the ΔT. The change of the height of the PBL between ground surface and free troposphere due to the change of the UHI effect is described in Fig. S6 of the SI. According to Fig. S6 (a)–(c), the PBL height decreased by ~3% in the winter, spring, and summer seasons, but this change of PBL height reached ~30% in autumn. The change in the UHI effect is expected to affect air pollution via atmospheric conditions (changes in the rate constants of atmospheric chemical reactions and changes in the mixing ratio of air due to the change of PBL height) and emissions (BVOC emissions from biogenic sources). These effects are discussed in the following sections.

https://doi.org/10.5194/egusphere-2024-1961
Preprint. Discussion started: 25 July 2024

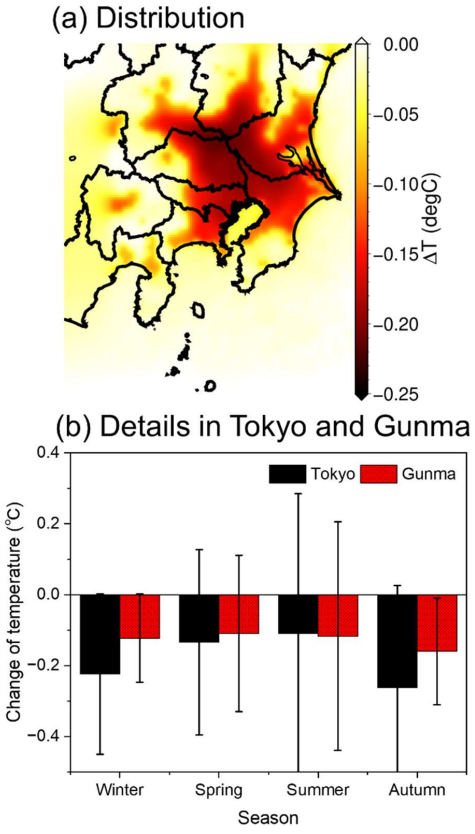

Figure 5: Changes in the ground temperature following the introduction of BEVs in the GTA: (a) yearly averaged distribution, and (b) seasonal variation in Tokyo and Gunma.

3.3 Effect of the introduction of BEVs on ground-level O_3 and $PM_{2.5}$ concentrations

3.3.1 Overall effects

Figure 6 shows the overall effects of introducing BEVs on the change in the yearly averaged O_3 and $PM_{2.5}$ concentrations in the GTA, which were evaluated by taking the difference in the results from the ALL and BASE scenarios. As shown in Fig. 6(a), O_3 increased around the central area of the GTA, as well as in several other sites for which consistent results were reported in a previous study (Hata et al., 2019; Kayaba and Kajino, 2023a). The seasonal changes in O_3 can be seen in Fig. S7 of the SI. According to the results, a strong increase in O_3 was estimated in the winter and autumn seasons, when a considerable decrease in temperature is estimated, affecting the UHI effect. However, a slight increase in O_3 in the spring and summer seasons

https://doi.org/10.5194/egusphere-2024-1961
Preprint. Discussion started: 25 July 2024

indicates that the UHI effect contributes significantly to the local formation of O_3 in the winter and autumn seasons. According to Fig. 6(b), increases in $PM_{2.5}$ also occurred on the western and northern sides of the GTA. The primary $PM_{2.5}$ emission was expected to decrease as a result of the introduction of BEVs; thus, this increase is attributed to the enhancement of secondary products. Seasonal changes in $PM_{2.5}$ are shown in Fig. S8 of the SI.

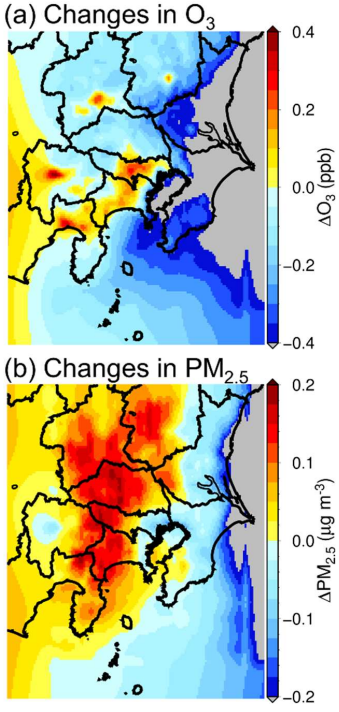

Figure 6: Change in the yearly-averaged (a) O_3 and (b) $PM_{2.5}$ concentrations following the introduction of BEVs in the GTA. Results include the effects of all BEV-introduction scenarios, including the reduction of primary air pollutants from the transport sector, increase in the primary air pollutants due to the high energy demands of battery charging, UHI mitigation, and changes in the BVOC emissions as a result of UHI mitigation.

3.3.2 Sensitivity analysis of the change in O_3

The contributions of the five scenarios that were subtracted from the BASE scenario: ALL, S_{EV}, S_{PP}, S_{UHI}, and S_{BVOC}, to changes in the O_3 concentrations in Tokyo and Gunma can be seen in Fig. 7. Detailed definitions of the scenarios are described in Sect. 2.3.3 and Table 1. According to Fig. 7, the seasonal trends obtained using the five scenarios were similar for Tokyo and Gunma, whereas the absolute change in O_3 was higher in Tokyo because of the condensed anthropogenic activities in the city. As mentioned in Sect. 3.3.1, the results of ALL show an increase in O_3 during winter and autumn and decreases in spring and summer, with S_{EV} also showing a decrease in O_3 for the summer season in Tokyo and Gunma. According to a previous

https://doi.org/10.5194/egusphere-2024-1961
Preprint. Discussion started: 25 July 2024

study (Kayaba and Kajino, 2023a), the atmospheric conditions in the urban area of the GTA are VOC-limited during summer; thus, the reduction of NO_X from vehicular emissions leads to an increase in O_3 over most of the year in Tokyo and Gunma. Regime analyses in Sect. 4.1 clarify the ozone sensitivity regime aside in seasons other than the summer. Furthermore, S_{PP}, S_{UHI}, and S_{BVOC} indicated negative impacts on the O_3 formation in Tokyo and Gunma in all seasons. The increase in air pollutants from power plants, mainly NO_X, leads to NO titration, lowering the O_3 concentration in Tokyo and Gunma. The power plants are located in the bay area of Tokyo; for which a detailed map is provided in a previous study (Kayaba and Kajino, 2023a). Notably, the mitigation effect of the UHI caused a significant decrease in the O_3 formation in Tokyo, which is attributed to the kinetics of O_3-chemistry and a lowered PBL height, indicating the importance of the introduction of BEVs to mitigate O_3 problems in urban areas, not only in terms of direct emissions but also the local temperature decrease. The UHI effect was considerably lower in Gunma than it was in Tokyo because Gunma is a suburban/rural site, and the decrease in temperature was not as significant in Gunma, as seen in Fig. 5. Mitigation of the UHI effect also caused a decrease in BVOC emissions in central GTA and an increase on the west side of the GTA. BVOCs have high O_3-formation potential; thus, the decrease in BVOC emissions in the center of the GTA lessened the O_3 concentration in Tokyo and Gunma. The results of the S_{UHI} and S_{BVOC} scenarios indicate that the introduction of BEVs mitigates the UHI effect, leading to the deactivation of both O_3 formation and BVOC emissions.

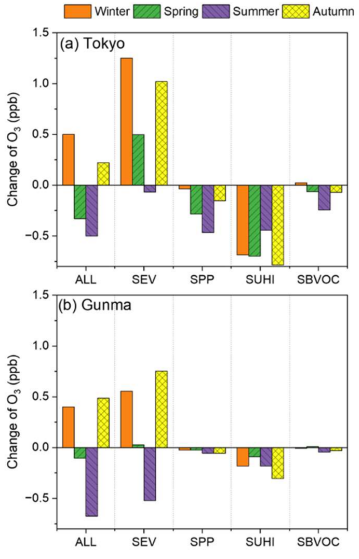

Figure 7: Contributions of the five scenarios to O_3 in (a) Tokyo and (b) Gunma.

https://doi.org/10.5194/egusphere-2024-1961
Preprint. Discussion started: 25 July 2024

3.3.3 Sensitivity analysis of changes in $PM_{2.5}$

Figure 8 shows the contributions of the five scenarios: ALL, S_{EV}, S_{PP}, S_{UHI}, and S_{BVOC}, to the observed change in the $PM_{2.5}$ concentration in Tokyo and Gunma. Unlike O_3, the seasonal trends in Tokyo and Gunma show different behaviors. The S_{EV} scenario negatively or slightly affected $PM_{2.5}$, owing to the decrease in primary emissions from the exhaust. S_{EV} positively affected $PM_{2.5}$ in Gunma, except during spring, while S_{PP}, S_{UHI}, and S_{BVOC} caused an increase in $PM_{2.5}$ in both Tokyo and Gunma over most of the year. The intense increase in $PM_{2.5}$ that was associated with S_{PP}, S_{UHI}, and S_{BVOC} is discussed in Sect. 4.2. Overall, unlike O_3, UHIs positively affect $PM_{2.5}$ formation, and changes to the UHI are likely to have negative effects on the GTA.

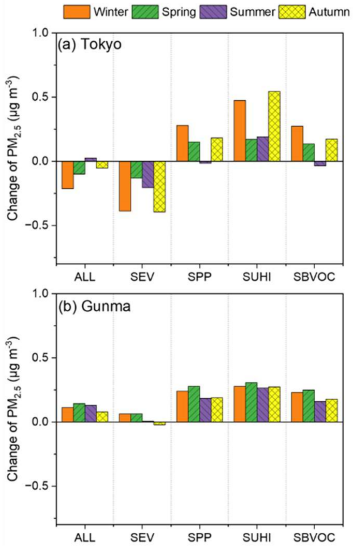

Figure 8: Contributions of the five scenarios to $PM_{2.5}$ in GTA in (a) Tokyo and (b) Gunma.

4 Discussion

4.1 Analysis of ozone formation sensitivity regime in the GTA

Figure 9 shows the seasonal average of the hydrogen peroxide (H_2O_2) to HNO_3 ratio (HNR) for the four seasons, each of which was averaged from 9 a.m. to 3 p.m. to represent the sensitivity of the daytime photochemical O_3 formation. Details of the HNR and related topics of O_3 formation-sensitive regimes are described in Appendix B. According to Fig. 9, the values of HNR around Tokyo are less than 0.5 for all seasons, meaning that the central Tokyo region of GTA is VOC-sensitive throughout the year. A relatively wide distribution of VOC-sensitive regimes was observed in spring, summer, and autumn, whereas a

https://doi.org/10.5194/egusphere-2024-1961
Preprint. Discussion started: 25 July 2024

narrow distribution was observed in the winter. According to Sect. 3.3.1 and 3.3.2, the sensitivity of the introduction of BEVs (scenario S_{EV}) to O_3 formation showed positive effects in winter and autumn. The value of ~0.1 for the HNR in Tokyo in winter and autumn indicates strong VOC sensitivity in Tokyo, and the decrease in the NO_X might surpass the effect of the VOC reduction, resulting in an increase in O_3 in the S_{EV} scenario for those seasons. Despite this, the degradation in the O_3 formation that results from the mitigation of the UHI effect contributed to reducing the effect of the increase in O_3, resulting in a mild increase in O_3 under the ALL scenario in winter and autumn. However, according to Fig. 9(b) and (c), the HNR was close to 0.5 for spring and summer, which is the border between the VOC-sensitive regime and NO_X-sensitive regime in and around central Tokyo. According to Sect. 3.3.1 and 3.3.2, the S_{EV} scenario results in a decrease in O_3 formation during spring and summer. Particularly in summer, Fig. 7 shows a decrease in O_3 under the S_{EV} scenario in both Tokyo and Gunma, despite the fact that Tokyo and Gunma are VOC-sensitive and transition regimes, respectively. This means that the effect of the VOC reduction might surpass the effect of the NO_X reduction in the warmer seasons, contributing to the decrease in O_3. Combined with the strong impact that UHI mitigation has as a result of the introduction of BEVs, O_3 was estimated to significantly decrease in the warmer seasons (ALL scenario). S_{PP}, the scenario used to confirm the effect of the increase in power plant emissions, also contributed to the decrease of O_3, similar to the UHI mitigation (S_{UHI} and S_{BVOC}). NO_X is the primary pollutant emitted by power plants. According to Fig. 9, central GTA was mostly VOC-limited, and the increase in NO_X emissions caused a decrease in O_3, leading to the observed decrease in O_3 in both Tokyo and Gunma under the S_{PP} scenario.

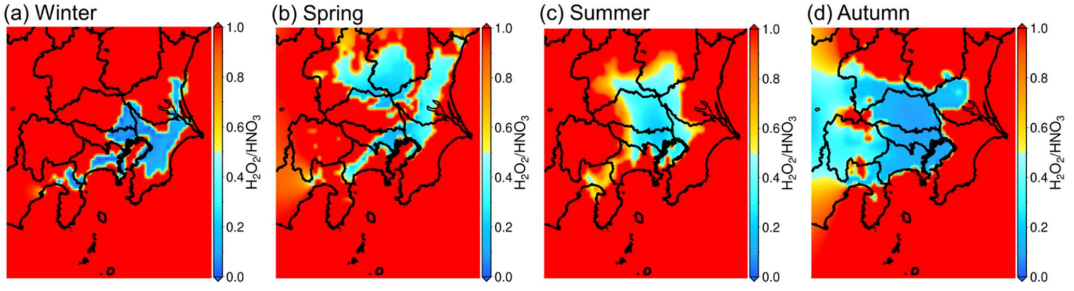

Figure 9: Seasonal trends in the ozone sensitivity regime defined by the ratio of H_2O_2/HNO_3 (HNR) for all four seasons. Analysis was conducted by averaging the results for 9: 00 a.m. to 3:00 p.m. each day. Values > 0.5 are NO_X-limited and < 0.5 are VOC-limited.

In addition to O_3 formation sensitivity, the effect of NO titration is important when discussing the impact of changes in primary emissions on direct O_3 formation (Akimoto et al., 2015). The concentration of total produced ozone, or potential ozone (PO), is defined using $[PO] = [O_3] + [TO]$. TO is the titrated-O_3 from NO titration with concentration defined by $[TO] = [NO_2]$-$\alpha[NO_X]$, where α is the ratio of O_3 formed by the reaction of $NO + O_3 \rightarrow NO_2$ (NO-titration). The parameter α is the ratio of O_3 that is scavenged by the titration of NO, for which a value of 0.1 has been widely accepted in Japan (Itano et al., 2007; Akimoto et al., 2015). Figure 10 shows the seasonal variation in the ratio of TO to PO (TO/PO), which exhibits the contribution of the NO titration effect to the total O_3 formation. The effect of NO titration is strong in the central area of Tokyo throughout the year because of high NO_X emissions and relatively high O_3 concentrations. Compared with the spring and summer, a wider

https://doi.org/10.5194/egusphere-2024-1961
Preprint. Discussion started: 25 July 2024

295 distribution of high TO/PO values is observed for winter and autumn, more relevant NO titration effects in these seasons. According to Fig. 7, a positive increase in O_3 was observed in winter and autumn with the introduction of BEVs, which might be partly attributed to the NO titration effect that results from NO_X-reduction.

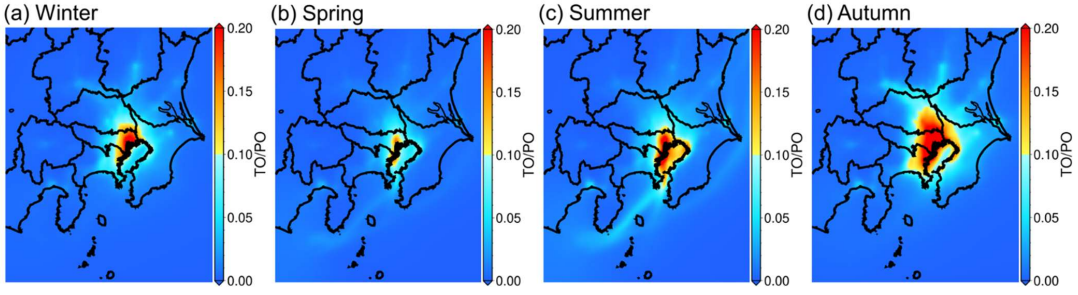

Figure 10: Seasonal trend in the effect of NO-titration defined by the ratio of titrated-O_3/potential-O_3 (TO/PO) for the four seasons.
300 **NO-titration is strong in regions where the value of TO/PO is high.**

4.2 Composition analysis of the change in $PM_{2.5}$ concentration resulting from the introduction of BEVs

The annual distributions of the four components of $PM_{2.5}$, NO_3^-(p), SO_4^{2-}(p), NH_4^+(p), and secondary organic aerosols (SOA) for the four sensitivity scenarios are shown in Fig. 11. In terms of S_{EV}, a large decrease in NO_3^-(p) was estimated due to the reduction in the primary emission of NO. On the other hand, SO_4^{2-}(p) increased because of the increase in the O_3 level,
305 enhancing the OH formation and increasing the SO_4^{2-}(p) that is attributed to the SO_2 + OH reaction. Increases in SO_4^{2-}(p) enhance SOA formation, leading to a large increase (Budisulistiorini et al., 2017). The S_{UHI} sensitivity scenario shows an increase in all components. It is well known that NO_3^-(p) is in equilibrium with HNO_3(g) in the atmosphere, and that the equilibrium shifts to the NO_3^-(p) form when the temperature increases, which is why a strong increase in NO_3^-(p) occurs in the S_{UHI} sensitivity scenario (Morino et al., 2006). The decrease in temperature that results from the introduction of BEVs in the
310 S_{UHI} scenario enhances the condensation of SOA, leading to an increase in the remaining components (Sheehan and Bowman, 2001). The most important result in the S_{BVOC} scenario is the increase in the components of $PM_{2.5}$ because changes in the UHI leads to changes in the BVOC in this scenario; however, because no temperature change was considered an increase in $PM_{2.5}$ was not expected. According to Fig. S4, the BVOC emissions decreased owing to changes in the UHI effect in similar regions, where an increase in the SO_4^{2-}(p) was observed, as seen in Fig. 11. This is unexpected because BVOC is considered a precursor
315 to SO_4^{2-}(p) in terms of OH generation. Possible reasons for this are discussed in Sect 4.3. The S_{EV} scenario also assumes the reduction of primary emissions, meaning that a decrease in SO_4^{2-}(p) was expected. Nevertheless, all components of $PM_{2.5}$, especially SO_4^{2-}(p) and SOA, were observed to increase considerably in the western and northern areas of the GTA, corresponding with the suburban to rural areas.

https://doi.org/10.5194/egusphere-2024-1961
Preprint. Discussion started: 25 July 2024

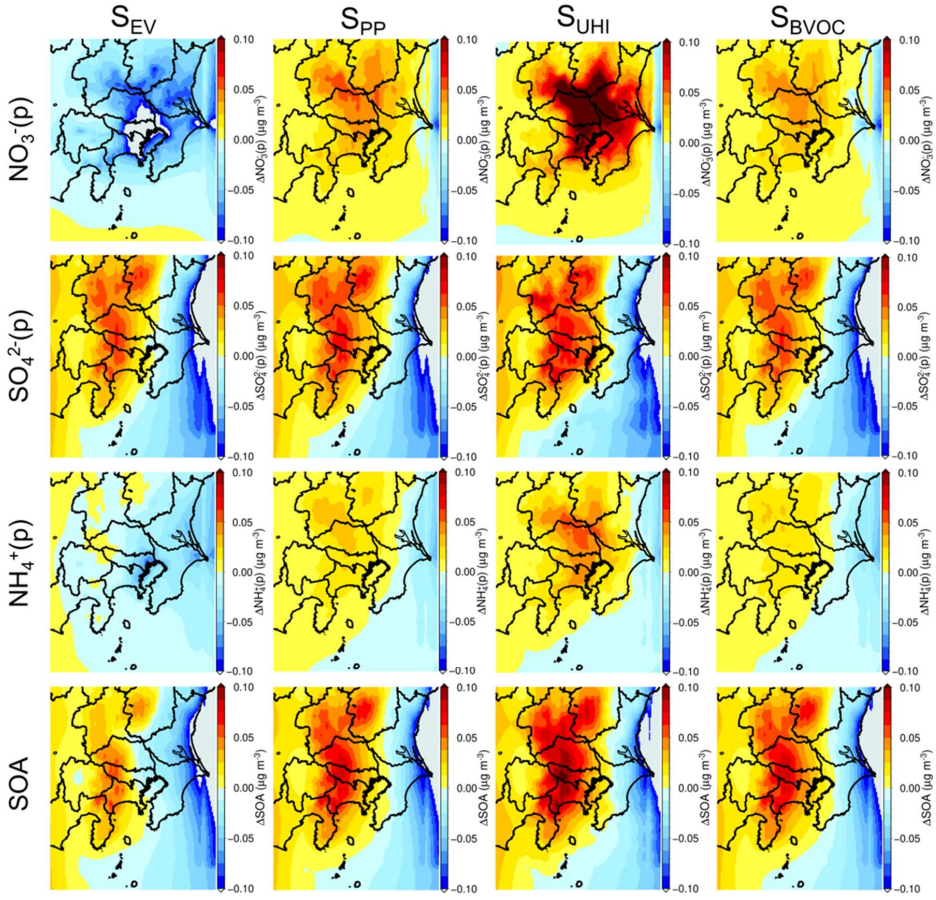

320 **Figure 11: Contributions of the four sensitivity scenarios to the annual average $PM_{2.5}$ composition in the GTA.**

4.3 Correlation between $PM_{2.5}$ increase, the change in BVOC emissions, and the UHI effect

The sensitivity scenarios for S_{BVOC} described in Sect. 4.2 showed an unreasonable increase in SO_4^{2-}(p) and a simultaneous increase in SOA. This indicates that not only the change in temperature and PBL height, but also the change in BVOC emissions caused by the mitigation of the UHI effect, led to increases in SO_4^{2-}(p) and SOA. According to Fig. S4, a decrease
325 in the BVOC emissions was observed in some parts of the central to northern regions of the GTA, with an increase observed in other areas. Considering the change in the BVOC emissions, the change in SO_4^{2-}(p) in the S_{BVOC} scenario can be explained by atmospheric-chemical discussions that are divided into daytime and nighttime, as seen in the following.

https://doi.org/10.5194/egusphere-2024-1961
Preprint. Discussion started: 25 July 2024

4.3.1 Sensitivity analysis of daytime $PM_{2.5}$ changes

First, considering the daytime S_{BVOC} scenario, the simplified oxidation reactions of BVOC and SO_2 are described in the following chemical reactions. BVOC oxidation by O_3 is not considered in this discussion because the rate of oxidation by OH is much faster than that associated with O_3.

$$BVOC + OH \rightarrow SOA \quad (R1)$$

$$SO_2 + OH \rightarrow SO_4^{2-}(p) \quad (R2)$$

In both R1 and R2, the particle formation schemes are simplified. The atmospheric oxidizer OH is generated by the following photochemical reactions during the daytime:

$$O_3 + h\nu \rightarrow O_2 + O(^1D) \quad (R3)$$

$$O(^1D) + H_2O \rightarrow 2OH \quad (R4)$$

Assuming a steady-state approximation of the intermediate radicals, the rates of $O(^1D)$ and OH are described by Eqs. 1 and 2:

$$\frac{d[O(^1D)]}{dt} = k_{R3}[O_3] - k_{R4}[O(^1D)][H_2O] = 0 \quad (1)$$

$$\frac{d[OH]}{dt} = 2k_{R4}[O(^1D)][H_2O] - k_{R1}[BVOC][OH] - k_{R2}[SO_2][OH] = 0 \quad (2)$$

where k_{R1}, k_{R2}, k_{R3}, and k_{R4} are the rate constants in Eq. R1, R2, R3, and R4 Combining Eqs. 1 and 2, the rate of $SO_4^{2-}(p)$ formation is described by Eq. 3, as follows:

$$\frac{d[SO_4^{2-}(p)]}{dt} = k_{R2}[SO_2][OH] = \frac{2k_{R2}k_{R3}[SO_2][O_3]}{k_{R1}[BVOC] + k_{R2}[SO_2]} \quad (3)$$

According to SAPRC-07 applied in the chemical transport model in this study, k_{R1} lies in the order ~10^{-11} cm^3 $molecule^{-1}$ s^{-1} and k_{R2} around ~10^{-13} cm^3 $molecule^{-1}$ s^{-1}. The BVOC concentration is much higher than the SO_2 concentration in suburban and rural areas, meaning that k_{R1}[BVOC] is much higher than $k_{R2}[SO_2]$. Thus, Eq. 3 can be transformed into Eqs. 4, as follows:

https://doi.org/10.5194/egusphere-2024-1961
Preprint. Discussion started: 25 July 2024

$$r_{SO4} \equiv \frac{d[SO_4^{2-}(p)]}{dt} = k_{R2}[SO_2][OH] = \frac{2k_{R2}k_{R3}[SO_2][O_3]}{k_{R1}[BVOC]} \quad (4)$$

According to Eq. 4, the rate of SO_4^{2-}(p) formation is proportional to O_3 and SO_2, and inversely proportional to BVOC. In terms of the chemical explanation, if BVOC emissions decrease due to changes in the UHI effect, the rate of reaction R1 is weakened; and the redundant OH enhances reaction R2, which is why r_{SO4} is inversely proportional to BVOC. According to Fig. 7, mitigation of the UHI effect led to a decrease in the O_3 in the S_{BVOC} scenario, degrading the chemical reaction, and the decrease in BVOC was caused by the mitigation of UHI via the introduction of BEVs. Therefore, if the rate of SO_4^{2-}(p) formation is calculated using Eq. 4, increases occur in the S_{BVOC} scenario as compared with the BASE scenario, indicating that SO_4^{2-}(p) formation is enhanced because the decrease in O_3 is lower than the decrease in BVOC. BVOC was assumed to be isoprene (because ~70 % of the BVOC emissions in Japan are isoprene (Hata et al., 2023)), and the ratio of r_{SO4} in BASE and S_{BVOC} ($\eta = r_{SO4}^{SBVOC}/r_{SO4}^{BASE}$) in daytime from 9:00 a.m. to 3:00 p.m. was calculated, with the results shown in Fig. 12(a). The η increases in the western and northern regions of GTA correspond to the distribution of the SO_4^{2-}(p) increase described in Fig. 11. More qualitatively, the reduction in the BVOC emissions reduced OH consumption, and the resulting OH enhanced SO_4^{2-}(p) formation in the western and northern regions of the GTA. Similarly, the decrease in primary emissions in the S_{EV} also led to a decrease in the NO_X and VOCs emissions, which might have enhanced the SO_2 + OH reaction, causing an increase in SO_4^{2-}(p) and ultimately enhancing the formation of SOA (Sheehan and Bowman, 2001).

4.3.2 Sensitivity analysis of nighttime $PM_{2.5}$ changes

The photochemical reactions R3 and R4 do not occur during the night, when OH is generated from different sources. One of the well-known sources of OH at night is alkene ozonolysis, leading to the formation of Criegee intermediates (CIs), and both the vibrationally excited and stabilized CIs form OH via unimolecular decomposition (Vereecken et al., 2017). These reaction pathways can be appended and described, as seen in reaction R5:

Alkene + O_3 → νOH (R5),

where ν is a stoichiometric number that depends on the type of alkene. Alkenes also consume OH radicals via reaction R6, and the rates of OH consumption by alkenes are higher than those of other types of VOCs, such as alkanes and aromatics.

Alkene + OH → SOA (R6).

SO_4^{2-}(p) is formed by reaction R2. Note that stabilized-CIs are also known to be strong oxidizers of SO_2 while the effect of SO_4^{2-}(p) formation from stabilized CIs is almost negligible in the GTA (Nakamura et al., 2023). The steady-state approximation of the OH formation rate is given by Eq. 7:

https://doi.org/10.5194/egusphere-2024-1961
Preprint. Discussion started: 25 July 2024

$$\frac{d[\mathrm{OH}]}{dt} = \nu k_{\mathrm{R5}}[\mathrm{Alkene}][\mathrm{O_3}] - k_{\mathrm{R6}}[\mathrm{Alkene}][\mathrm{OH}] - k_{\mathrm{R2}}[\mathrm{SO_2}][\mathrm{OH}] = 0 \qquad (7)$$

where k_{R5} and k_{R6} are the rate constants of R5 and R6, respectively. Coupled with reaction R2, nighttime r_{SO4}, assuming simply that $\nu = 1$, is formulated as follows:

$$\frac{d[\mathrm{SO_4^{2-}(p)}]}{dt} = k_{\mathrm{R2}}[\mathrm{SO_2}][\mathrm{OH}] = \frac{2k_{\mathrm{R2}}k_{\mathrm{R5}}[\mathrm{Alkene}][\mathrm{SO_2}][\mathrm{O_3}]}{k_{\mathrm{R1}}[\mathrm{Alkene}] + k_{\mathrm{R2}}[\mathrm{SO_2}]} \qquad (8)$$

Assuming [Alkene] >> [SO_2] in the countryside, Eq. 8 can be transformed into Eq. 9 as follows:

$$r_{\mathrm{SO4}} \equiv \frac{d[\mathrm{SO_4^{2-}(p)}]}{dt} = k_{\mathrm{R2}}[\mathrm{SO_2}][\mathrm{OH}] = \frac{2k_{\mathrm{R2}}k_{\mathrm{R3}}}{k_{\mathrm{R1}}}[\mathrm{SO_2}][\mathrm{O_3}] \qquad (9)$$

Thus, nighttime r_{SO4} is directly proportional to the concentration of O_3. Chemically, nighttime alkene ozonolysis increases the number of OH radicals through CI-chemistry, indicating that O_3 concentration is the key factor for OH concentration and r_{SO4}. The value of η (= $r_{\mathrm{SO4}}^{\mathrm{SBVOC}}/r_{\mathrm{SO4}}^{\mathrm{BASE}}$) in nighttime from 9:00 p.m. to 3:00 a.m. was calculated using Eq. 9, and the results shown in Fig. 12(b). The fact that η takes a value of > 1.0 in central to north regions of GTA means that r_{SO4} will increase in S_{BVOC} for most of the GTA. The increase in nighttime r_{SO4} is almost equivalent to the increase in daytime r_{SO4}, and r_{SO4} increases in the S_{BVOC} scenario compared with BASE in both daytime and nighttime. As mentioned in Sect. 4.3.1, similar arguments can be made for the S_{EV} scenario, where OH is treated as the source for the oxidation of alkenes. The nitrate radical (NO_3) that is formed by the reaction of NO_2 and O_3 is also known as an important oxidizer of alkenes at night (Ng et al., 2017). NO_3 adducts the C=C double bond of alkenes, finally forming organic peroxides (RO_2), which affect the nocturnal HO_X cycle. For this reason, the reaction of alkenes with NO_3 is also expected to enhance OH formation and subsequent SO_2 oxidation; however, discussion of NO_3 is omitted in this study for simplicity. As a conclusion of Sect. 4.3, mitigation of the UHI caused an increase in SO_4^{2-}(p) and subsequent $PM_{2.5}$ formation; however, the change in the UHI affected the BVOC emissions in the GTA, and the decrease in BVOC emissions itself also caused an increase in the SO_4^{2-}(p) formation due to enhancement of the SO_2 + OH reaction.

https://doi.org/10.5194/egusphere-2024-1961
Preprint. Discussion started: 25 July 2024

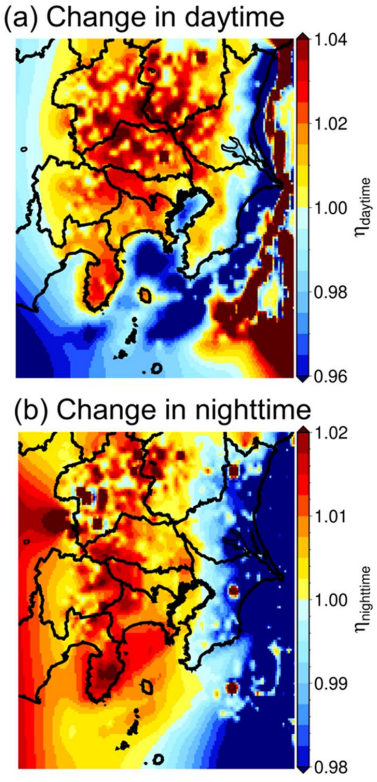

Figure 12: Annual mean ratio of r_{SO4}, $\eta = r_{SO4}^{SBVOC}/r_{SO4}^{BASE}$ obtained by BASE and S_{BVOC} for (a) daytime from 9:00 a.m. to 3:00 p.m., and (b) nighttime from 9:00 p.m. to 3:00 a.m.

4.4 Impact of the introduction of BEVs on premature mortality

Previous sections have suggested that the introduction of BEVs in the GTA leads to an increase in O_3 in the urban area and an increase in $PM_{2.5}$ in the suburban/rural area. To evaluate how these effects impact human health, the changes in premature mortality that resulted from changes in O_3 and $PM_{2.5}$ were estimated. The change in the number of deaths, ΔP, was calculated using Eq. 5, as follows:

$$\Delta P = \mathrm{sgn}(\Delta C) \cdot \left(1 - e^{-\beta|\Delta C|}\right) \cdot P_d \qquad (5)$$

where sgn is a sign function, ΔC is the change in concentration of air pollutants, and P_d is the base number of deaths in the calculated region. β is an epidemiological parameter that is defined by Eq. 6, as follows:

https://doi.org/10.5194/egusphere-2024-1961
Preprint. Discussion started: 25 July 2024

$$\beta = \frac{\ln(\mathrm{RR})}{\Delta C_{\mathrm{RR}}} \quad (6)$$

where RR is the relative risk from exposure to air pollutants and ΔC_{RR} is the change in the concentration of a pollutant. Values of 1.003 for MDA8 O_3 change and 1.04 for daily average $PM_{2.5}$ with ΔC_{RR} = 10 μg m^{-3} were used in this study (Poppe III et al., 2002; WHO Regional Office for Europe, 2008). The calculated target was the changes before and after the introduction of BEVs (the ALL scenario) for the entire region of the GTA (D3 in Fig. 1). The results showed that the change in the number of deaths caused by the change in O_3 concentration was -175 (-1.41 × 10^{-4} % of the total population), while the changes in the $PM_{2.5}$ concentration led to a decrease of -77 (-6.21 × 10^{-5} % of the total), indicating that the number of deaths decreased after the introduction of BEVs with regards to both O_3 and $PM_{2.5}$. Premature mortality in association with changes in O_3 after the introduction of BEVs has been estimated previously for the urban part of the GTA; however, the effects in the rural area were not considered (Hata et al., 2019). According to the results of this study, the O_3-related premature deaths over the entire GTA following the introduction of BEVs saved 175 lives in the region. Furthermore, $PM_{2.5}$ concentration increases were observed mainly in the suburban/rural areas, which is due to the change in kinetics before and after the introduction of BEVs. Nevertheless, the population is condensed within the urban areas, where the estimated decrease in $PM_{2.5}$ was due to the decrease in primary emissions, and 77 deaths were prevented in the GTA. Therefore, the introduction of BEVs in the GTA is effective, not only in supporting GHG emission issues but also in mitigating the health impacts that result from air pollution. The change in UHI after the introduction of BEVs is one of the most important factors in the change in O_3 and $PM_{2.5}$. Nevertheless, it should be noted that in terms of $PM_{2.5}$, 122 more premature deaths were estimated for rural/suburban areas due to the increase in $PM_{2.5}$, mainly because of changes in the UHI and the increase in emissions from power plants, indicating that local health risks are likely to be induced by the introduction of BEVs.

5 Summary

The impacts of the introduction of BEVs on ground-level O_3 and $PM_{2.5}$ were evaluated by chemical transport modeling in the GTA, with a particular focus on the effect of the change in UHI. The results suggest O_3 increases in urban areas and $PM_{2.5}$ increases in suburban/rural areas. The change in the UHI contributed to a decrease in O_3 formation due to the degradation of O_3-related atmospheric chemistry, while it contributed to an increase in $PM_{2.5}$ due to the enhancement of particle condensation and, in some regions, a decrease in BVOCs, which led to the enhancement of SO_4^{2-}(p) formation. The change in the number of premature deaths after introducing BEVs was calculated to be -175 in association with O_3 and -77 for $PM_{2.5}$ over the entire GTA, suggesting positive impacts on human health. Previous studies have mainly focused on the effects of the decrease in primary emissions due to the shift from ICVs to BEVs on ground-level O_3; however, no studies have shown clear evidence of how the mitigation of the UHI by the introduction of BEVs has a local impact on O_3 and $PM_{2.5}$. This study showed the relevant

https://doi.org/10.5194/egusphere-2024-1961
Preprint. Discussion started: 25 July 2024

impact of UHI mitigation on the decrease in O_3 and increase in $PM_{2.5}$, for which the absolute contributions were as high as the change in primary emissions. Despite these findings, this study only focused on road transportation; however, a similar treatment could be considered for all stationary sources and other transportation vehicles such as ships, to clarify how electrization changes the local UHI effect its effect on air pollution. Finally, this study focused on 2017, but the entire transformation from ICVs to BEVs is expected to reach completion, such as the 2050s, when the atmosphere will have changed; thus, the O_3 formation sensitivity regime will also differ. Future research should therefore implement emission inventories and meteorology for different time periods to comprehensively evaluate the effect of emission strategies and the UHI effect.

Appendix A: Estimation of the changes in anthropogenic heat as a result of converting ICVs to BEVs in 2017

A.1 Modelled vehicles

Tables A1 and A2 show the specifications of the modeled vehicles used to estimate the change in anthropogenic heat after substitution with BEVs. Three types of vehicles were compared in this study: light passenger cars, normal passenger cars, and small heavy-duty vehicles. Each type of vehicle was compared, and the same model used for ICVs and BEVs, with differences thus primarily involving the energy source (engine or battery). Based on the differences between ICVs and BEVs listed in Tables A1 and A2, the change in anthropogenic heat was estimated as described in the following sections.

Table A3: Specifications of passenger cars modeled in this study (L/100 km for ICVs and Wh/km for BEVs).

Property	Light passenger car		Normal passenger car	
Category	Conventional	BEV	Conventional	BEV
Manufacturer	Nissan	Nissan	Toyota	Nissan
Model	SBA-B43W	ZAA-B6AW	BA-MZEA17W-AWXNB	ZAA-ZE1
Total weight (kg)	1060	1290	1535	1795
WLTC (L/100km and Wh/km)*	4.31	124	5.24	155
Urban (L/100km and Wh/km)*	5.15	100	7.35	133
Rural (L/100km and Wh/km)*	4.02	113	5.03	145
Highway (L/100km and Wh/km)*	4.15	142	4.46	171

Table A2: Specifications of small heavy-duty vehicles modeled in this study (L/100km for ICV and Wh/km for BEV).

Property	Small heavy-duty vehicle	
Category	Conventional	BEV
Manufacturer	Mitsubishi	Mitsubishi

https://doi.org/10.5194/egusphere-2024-1961
Preprint. Discussion started: 25 July 2024

Model	2RG-FBAV0	ZAB-FEAVK
Total weight (kg)	4495	5015
JH25 (L/100km and Wh/km)*	8.46	347

A.2 Estimation of the changes in exhaust emissions for the three types of vehicles

The change in the emissions of primary air pollutants due to the substitution of ICVs with BEVs was estimated by multiplying the emission factors with the sources of engine exhaust emissions, evaporative emissions from vehicles (hot-soak loss, diurnal breathing loss, and running loss), and evaporative emissions from gasoline service stations as defined in the emission inventory provided by the Ministry of the Environment (Shibata and Morikawa, 2021). Light and normal passenger cars and small heavy-duty ICVs were assumed to be substituted by BEVs. The emissions from engine exhaust, evaporation from vehicles, and evaporation from service stations were set to zero by multiplying the emission factor of 0 by the emission inventories. The primary emissions of particles from brake and tire dust were not examined in this study.

A.3 Estimation of the change of primary emissions from powerplants in GTA

The change in the emissions of primary air pollutants from power plants as a result of substituting ICVs with BEVs was estimated based on the catalog data of the three BEVs listed in Tables A1 and A2, statistical data of the number of vehicles in the GTA (Database from Automobile Inspection & Registration Information Association, 2024) and the average mileage per year (Ministry of Land, Infrastructure, Transport, and Tourism, 2024) listed in Table A3.

Table A3: Number of vehicles in GTA and the average mileage per year set in this study.

Category	Number of vehicles	Mileage (km/y)
Light passenger	11 286 521	10 575
Normal passenger	6 181 929	10 575
Small HV	3 053 453	14 325

Multiplying the number of vehicles in the GTA, mileage per year, and battery consumption listed in Tables A1 and A2 by the transmission loss of electricity from power plants to charging stations (1.038) resulted in a total energy demand of 49.6 TWh/y for charging BEVs in the GTA. The total energy demand for electricity in the GTA in 2017 was estimated at 147 TWh/y. Thus, the energy demand in powerplants in GTA after substituting ICVs with BEVs increased $49.6/147 \times 100 = 34$ %, and we assumed that the increase in the primary emissions of air pollutants from powerplants was proportional, at 34 %, in the BEV-introduction scenario.

https://doi.org/10.5194/egusphere-2024-1961
Preprint. Discussion started: 25 July 2024

A.4 Estimation of the change in AH for the three types of vehicles

The change in anthropogenic heat caused by substituting ICVs with BEVs was estimated for each vehicle type based on the energy efficiencies listed in Tables A1 and A2. The thermal enthalpies of gasoline (passenger cars) and light fuel (small heavy-duty vehicles) ICVs were assumed to be 31 250 kJ/L and 35 770 kJ/L, respectively (Agency for Natural Resources and Energy, 2024), allowing the ratio of AH between the ICVs and BEVs to be calculated. For example, the fuel consumption of conventional light passenger cars listed in Table A1 was 5.15 L/100 km. Multiplying the gasoline thermal enthalpy (31250 kJ/L by 5.15 L/100 km, results in a total energy consumption of 1347 kJ/km. The battery consumption of the light passenger car BEV listed in Table A1 is 124 Wh/km = 446 kJ/km. Thus, the ratio of the decrease in AH caused by the introduction of light passenger BEVs was calculated to be 446/1347 = 0.33. Similarly, the ratios of the decrease in AH by the introduction of BEV normal passenger cars and small heavy-duty vehicles were calculated to be 0.34 and 0.41 respectively. Then, by applying statistical data on the number of vehicles (Database from Automobile Inspection & Registration Information Association, 2024) listed in Table A3, the number-weighted ratio of the decrease in AH was calculated to be 0.35. This indicates that the change in AH before and after the introduction of BEVs contributed to the 35 % decrease.

The Ministry of the Environment released the estimated data of UHI-related parameters, including AH, from stationery and transportation sources for the metropolitan area of Tokyo (Ministry of the Environment, 2010). According to this report, the AH from the transportation sector was 505.8 TJ/d, and the AH from all sectors was 1574.3 TJ/d. This study focuses on the electrification of passenger cars and small heavy-duty vehicles, and the ratio of the number of these vehicles in GTA is 89 %, meaning that the AH from the targeted vehicles is calculated at 505.8 × 0.892 = 451.5 TJ/d. The ratio of the decrease in the AH after the introduction of BEVs was calculated to be 0.35; therefore, the decrease in AH after the introduction of BEVs is 505.8 × 0.892 × 0.35 = 157.6 TJ/d, and the AH after the introduction of BEVs in the transportation sector is 505.8 – 451.5 + 157.6 = 211.9 TJ/d. The AH from all sectors after the introduction of BEVs is calculated to be 1574.3 – 505.8 + 211.9 = 1280.4 TJ/d. Finally, the ratio of the decrease in the total AH after the introduction of BEVs was calculated to be 1280.4 / 1574.3 = 0.813. Therefore, a total decrease of 81.3 % AH is assumed for the GTA as a result of introducing BEVs under the assumptions made in these discussions.

Appendix B: Details of methods used to determine the ozone formation sensitivity regime

The formation of O_3 is dependent on the concentration of NO_X, and the rate of O_3 formation is determined by the concentration of VOCs. The balance of NO_X and VOCs concentrations thus determines whether O_3 formation is positive or negative when emission reduction strategies are implemented. Atmospheric conditions in high-NO_X regions, such as highly urbanized areas, are considered VOC-limited, while conditions in high-VOC regions such as forest, are NO_X-limited (Sillman, 1999). In the VOC-limited regime, the reduction in VOC emissions responded to a decrease in O_3 whereas the reduction in NOx emissions responded to an increase in O_3. In contrast, in the NO_X-limited regime, a reduction in the NO_X emissions corresponded to a decrease in O_3, with almost no response to VOC in terms of O_3 formation. Several indicators enabled the determination of the

https://doi.org/10.5194/egusphere-2024-1961
Preprint. Discussion started: 25 July 2024

O_3-sensitivity regime in the targeted region. For example, the formaldehyde (HCHO) to NO_2 ratio (FNR) is commonly used to distinguish between VOC-sensitive (FNR < 1.0), NO_X-sensitive (FNR > 2.0), and transition regimes (1.0 ≤ FNR ≤ 2.0) (Tonnesen and Dennis, 2000; Martin et al., 2004; Duncan et al., 2010). The analytical hypothesis of the FNR came from the fact that HCHO is an intermediate product of atmospheric oxidation; thus, the amount of HCHO can be an indicator of VOC. FNR is commonly used in several studies, especially because of the availability of data on the column density of HCHO and NO_2 from satellites such as the Ozone Monitoring Instrument (Vander, 2010) and TROPOspheric Monitoring Instrument (van Geffen et al., 2020). Nevertheless, HCHO is produced not only by the oxidation of VOCs, but also by primary emission, and the value of the FNR strongly depends on the location (Jin et al., 2017). In addition to FNR, the hydrogen peroxide (H_2O_2) to HNO_3 ratio (HNR) has been proposed as an indicator of the ozone sensitivity regime (Sillman, 1995). The analytical hypothesis of the HNR was based on the fact that both H_2O_2 and HNO_3 are end products of the HO_X cycle and are produced via the termination reaction of two OH radicals to form H_2O_2 and the reaction of OH and NO_2 to form HNO_3. According to Kayaba et al., regimes are distinguished as VOC-sensitive (HNR < 0.5) and NO_X-sensitive (HNR > 0.5) in the GTA (Kayaba et al., 2023a). Unlike the FNR, the HNR does not directly depend on primary emissions; therefore, an accurate analysis can be performed without considering location. Therefore, in this study, HNR was used to discuss the O_3 sensitivity regime.

Data availability

All the data simulated I this study are available upon request from the corresponding author.

Competing interests

The authors declare that they have no conflict of interest.

Acknowledgements

This study was supported by the Keidanren (Japan Business Federation) Foundation for Environmental Protection Measures. We thank Dr. Masayuki Hara at Kochi University for providing us with the urban canopy parameters for the WRF calculations. We also thank Dr. Yuya Takane of the National Institute of Advanced Industrial Science and Technology for the initial assistance with WRF calculations coupled with the urban canopy model.

Author contributions

HH and TI proposed the research concept. NM calculated the energy consumption and anthropogenic heat from the data of conventional and electric vehicles. HH performed the numerical simulations and analyses and drafted the manuscript. NM and TI reviewed the manuscript for accuracy.

https://doi.org/10.5194/egusphere-2024-1961
Preprint. Discussion started: 25 July 2024

References

560 Akimoto, H., Mori, Y., Sasaki, K., Nakanishi, H., Ohizumi, T., Itano, Y. Analysis of monitoring data of ground-level ozone in Japan for long-term trend during 1990–2010: Causes of temporal and spatial variation. Atmos. Environ., 102, 302–310, https://doi.org/10.1016/j.atmosenv.2014.12.001, 2015.

Agency for Natural Resources and Energy. Standard enthalpy and the emission factors of carbon dioxide from energy sectors. https://www.enecho.meti.go.jp/statistics/total_energy/pdf/stte_028.pdf (accessed April 19, 2024, in Japanese).

565 Andersson, Ö., Börjesson, Pal. The greenhouse gas emissions of an electrified vehicle combined with renewable fuels: Life cycle assessment and policy implications. Appl. Energy, 289, 116621, https://doi.org/10.1016/j.apenergy.2021.116621, 2021.

Binkowski, S.F.; Roselle, J.S. Models-3 community Multiscale Air Quality (CMAQ) model aerosol component 1. Model description. J. Geophys. Res. Atmos., 108(D6), 4183, https://doi.org/10.1029/2001JD001409, 2003.

570 Budisulistiorini, S.H., Nenes, A., Cariton, G.A., Surratt, J.D., McNeill, V.F., Pye, H.O.T. Simulating aqueous-phase isoprene-epoxydiol (IEPOX) secondary organic aerosol production during the 2013 Southern Oxidant and Aerosol Study (SOAS). Environ. Sci. Technol., 51(9), 5026–5034, https://doi.org/10.1021/acs.est.6b05750, 2017.

Carter, W.P.L. Development of the SAPRC-07 chemical mechanism. Atmos. Environ., 44(40), 5324–5335, https://doi.org/10.1016/j.atmosenv.2010.01.026, 2010.

575 Database from Automobile Inspection & Registration Information Association. https://airia.or.jp/ (accessed April 11, 2024, in Japanese).

Casals, C.L., Martinez-Laserna, E., Garcia, A.B., Nieto, N. Sustainability analysis of the electric vehicle use in Europe for CO_2 emissions reduction. J. Clean. Prod., 127, 425–437, https://doi.org/10.1016/j.jclepro.2016.03.120, 2016.

Chatani, S., Yamaji, K., Sakurai, T., Itahashi, S., Shimadera, H., Kitayama, K., Hayami, H. Overview of model inter-
580 comparison in Japan's study for reference air quality modeling (J-STREAM). Atmosphere, 9(1), 19, https://doi.org/10.3390/atmos9010019, 2018.

Dubash, N.K., Khosla, R., Kelkar, U., Lele, S. India and climate change: evolving ideas and increasing policy engagement. Annu. Rev. Environ. Resour., 43, 395–424, https://doi.org/10.1146/annurev-environ-102017-025809, 2018.

Duncan, N.B., Yoshida, Y., Olson, R. J., Sillman, S., Martin, V.R., Lamsal, L., Hu, Y., Pickering, E.K., Retscher, C., Allen,
585 J.D., Crawford, H.J. Application of OMI observations to a space-based indicator of NO_X and VOC controls on surface ozone formation. Atmos. Environ., 44(18), 2213-2223, https://doi.org/10.1016/j.atmosenv.2010.03.010, 2010.

Emery, C., Liu, Z., Russell, G.A., Odman, T.M., Yarwood, G., Kumar, N. Recommendations on statistics and benchmarks to assess photochemical model performance. J. Air Waste Manag. Assoc., 67(5), 582–598, https://doi.org/10.1080/10962247.2016.1265027, 2017.

590 Fawzy, S., Osman, A.I., Doran, J., Rooney, D.W. Strategies for mitigation of climate change: a review. Environ. Chem. Lett., 18(6), 2069–2094, https://doi.org/10.1007/s10311-020-01059-w, 2020.

https://doi.org/10.5194/egusphere-2024-1961
Preprint. Discussion started: 25 July 2024

Ferero, E., Alessandrini, S., Balanzino, A. Impact of the electric vehicles on the air pollution from a highway. Appl. Energy, 169, 450–459, https://doi.org/10.1016/j.apenergy.2016.01.098, 2016.

Finlayson-Pitts, J.B., Pitts Jr. N.J. Atmospheric chemistry of tropospheric ozone formation: Scientific and regulatory implications. Air & Waste, 43(8), 1091–1100, https://doi.org/10.1080/1073161X.1993.10467187, 1993.

Forrest, K., Kinnon, M.M., Tarroja, B., Samuelsen, S. Estimating the technical feasibility of fuel cell and battery electric vehicles for the medium and heavy duty sectors in California. Appl. Energy, 276, 115439, https://doi.org/10.1016/j.apenergy.2020.115439, 2020.

Fox, M., Zuidema, C., Bauman, B., Burke, T., Sheehan, M. Integrating public health into climate change policy and planning: state of practice update. Int. J. Environ. Res. Public Health, 16(18), 3232, https://doi.org/10.3390/ijerph16183232, 2019.

Hara, M., Kusaka, H., Kimura, F. Effect of global climate change on urban heat island intensity of Tokyo metropolitan area: winter season case. Nagare: Journal of Japan Society of Fluid Mechanics, 29(5), 353–361, 2010.

Hata, H., Tonokura, K. Impact of next-generation vehicles on tropospheric ozone estimated by chemical transport model in the Kanto region of Japan. Sci. Rep., 9, 3573, 2019.

Hata, H., Inoue, K., Kokuryo, K., Tonokura, K. Detailed inventory of the evaporative emissions from parked gasoline vehicles and an evaluation of their atmospheric impact in Japan. Environ. Sci. Technol., 54(10), 5947–5953, 2020.

Hata, H., Inoue, K., Yoshikado, H., Genchi, Y., Tsunemi, K. Impact of introducing net-zero carbon strategies on tropospheric ozone (O_3) and fine particulate matter ($PM_{2.5}$) concentrations in Japanese region in 2050. Sci. Total Environ., 891, 164442, http://id.ndl.go.jp/bib/10905806, 2023.

Heidari, N., Pearce, J.M. A review of greenhouse gas emission liabilities as the value of renewable energy for mitigating lawsuits for climate change related damages. Renew. Sust. Energ. Rev., 55, 899–908, https://doi.org/10.1016/j.rser.2015.11.025, 2016.

Holmes, S.N. A review of particle formation events and growth in the atmosphere in the various environments and discussion of mechanistic implications. Atmos. Environ., 41(10), 2183–2201, https://doi.org/10.1016/j.atmosenv.2006.10.058, 2007.

Hosseinzadeh-Bandbafha, H., Rafiee, S., Mohammadi, P., Ghobadian, B., Lam, S.S., Tabatabaei, M., Aghbashlo, M. Exergetic, economic, and environmental life cycle assessment analyses of a heavy-duty tractor diesel engine fueled diesel-biodiesel-bioethanol blends. Energy Convers., 241, 114300, https://doi.org/10.1016/j.enconman.2021.114300, 2021.

Iacobuta, G., Dubash, N.K., Upadhya, P., Deribe, M., Höhne, N. National climate change mitigation legislation, strategy and targets: a global update. Clim. Policy, 18(9), 1114–1132, https://doi.org/10.1080/14693062.2018.1489772, 2018.

Itano, Y., Bandow, H., Takenaka, N., Saitoh, Y., Asayama, A., Fukuyama, J. Impact of NO_X reduction on long-term ozone trends in an urban atmosphere. Sci. Total Environ. 379, 46–55, https://doi.org/10.1016/j.scitotenv.2007.01.079, 2007.

Jin, X., Fiore, M.A., Murray, T.L., Valin, C.L., Lamsal, B., Duncan, K., De Smedt, I.B.F., Abad, G.G., Chance, K., Tonnesen, S.G. Evaluating a space-based indicator of surface ozone-NOx-VOC sensitivity over midlatitude source regions and application to decadal Trends. J. Geophys. Res. Atmos., 122, 10439–10461, https://doi.org/10.1002/2017JD026720, 2017.

https://doi.org/10.5194/egusphere-2024-1961
Preprint. Discussion started: 25 July 2024

Kayaba, S., Kajino, M. Potential impact of battery electric vehicle penetration and changes in upstream process emissions assuming night-charging on summer O_3 concentration in Japan. J. Geophys. Res. Atmos., 128(11), e2022JD037578, https://doi.org/10.1029/2022JD037578, 2023a.

Kayaba, S., Kajino, M. Potential impacts of energy and vehicle transformation through 2050 on oxidative stress-inducing $PM_{2.5}$ metals concentraion in Japan. GeoHealth, 7(10), e2023GH000789, 2023b. https://doi.org/10.1029/2023GH000789.

Japan Meteorological Agency archives. https://www.jma.go.jp/jma/indexe.html (accessed April 11, 2024).

Kusaka, H., Kondo, H., Kikegawa, Y., Kimura, F. A simple single-layer urban canopy model for atmospheric models: Comparison with multi-layer and slab models. Boundary Layer Meteorol., 101, 329–358, https://doi.org/10.1023/A:1019207923078, 2001.

Li, C., Cao, Y., Zhang, Mi., Wang, J., Liu, J., Shi, H., Geng, Y. Hidden benefits of electric vehicles for addressing climate change. Sci. Rep., 5, 9213, https://doi.org/10.1038/srep09213, 2015.

Li, N., Chen, J.-P., Tsai, I-C., He, Q., Chi, S.-Y., Lin, Y.-C., Fu, T.-M. Potential impacts of electric vehicles on air quality in Taiwan. Sci. Total Environ. 566-567, 919–928, https://doi.org/10.1016/j.scitotenv.2016.05.105, 2016.

Lin, W.-Y., Hsiao, M.-C., Wu, P.-C., Fu, S.J., Lai, L.-W., Lai, H.-C. Analysis of air quality and health co-benefits regarding electric vehicle promotion coupled with power plant emissions. J. Clean. Prod. 247, 119152, https://doi.org/10.1016/j.jclepro.2019.119152, 2020.

Marin, V.R., Fiore, M.A., Van Donkelaar, A. Space-based diagnosis of surface ozone sensitivity to anthropogenic emissions. Geophys. Res. Lett., 31(6), https://doi.org/10.1029/2004GL019416, 2004.

Ministry of Land, Infrastructure, Transport, and Tourism. Data of the actual use of road transportation. https://www.mlit.go.jp/jidosha/iinkai/seibi/5th/5-2.pdf (accessed April 11, 2024, in Japanese).

Ministry of the Environment. Inventory of urban anthropogenic heat. https://www.env.go.jp/air/report/h16-05/chpt01.pdf (accessed April 11, 2024, in Japanese).

Morino, Y., Kondo, Y., Takegawa, N., Miyazaki, Y., Kita, K., Komazaki, Y., Fukuda, M., Miyakawa, T., Moteki, N., Worsnop, R.D. Partitioning of HNO_3 and particulate nitrate over Tokyo: Effect of vertical mixing. J. Geophys. Res. Atmos., 111, D15215, https://doi.org/10.1029/2005JD006887, 2006.

Moro, A., Lonza, L. Electricity carbon intensity in European Member States: Impacts on GHG emissions of electric vehicles. Transp. Res. D Transp. Environ., 64, 5–14, https://doi.org/10.1016/j.trd.2017.07.012, 2018.

Mulrow, J., Grubert, E. Greenhouse gas emissions embodied in electric vehicle charging infrastructure: a method and case study of Georgia, US 2021-2050. Enriron. Res.: Infrastruct. Sustain., 3, 015013, https://doi.org.10.1088/2634-4505/acc548, 2023.

Muratori, M. Impact of uncoordinated plug-in electric vehicle charging on residential power demand. Nat. Energy, 3, 193–201, https://doi.org/10.1038/s41560-017-0074-z, 2018.

Murphy, B.N., Nolt, G.C., Sidi. F, Bash, O.J., Appel, W.K, Jang, C., Kang, D., Kelly, J., Mathur, R.,Napelenok, S.,Pouliot, G., Pye, T.O.H. The detailed emissions scaling, isolation, and diagnostic (DESID) module in the community multiscale air

https://doi.org/10.5194/egusphere-2024-1961
Preprint. Discussion started: 25 July 2024

quality (CMAQ) modeling system version 5.3.2. Geosci. Model Dev., 14, 3407–3420, https://doi.org/10.5194/gmd-14-3407-2021, 2021.

Nakamura, Y., Hata, H., Tonokura, K. Urban-scale analysis of the seasonal trend of stabilized-Criegee intermediates and their effect on sulphate formation in the Greater Tokyo Area. Environ. Sci.: Atmos., 3, 1758–1766, https://doi.org/10.1039/D3EA00105A, 2023.

National Center for Atmospheric Research archives. NCEP FNL Operational Model Global Tropospheric Analyses, continuing from July 1999. 10.5065/D6M043C6 (accessed April 11, 2024).

National Oceanic and Atmospheric Administration. Environmental Modeling Center archives. https://polar.ncep.noaa.gov/sst/ (accessed April 11, 2024).

Ng, L.N.; Brown, S.S., Archibald, T.A., Atlas, E., Cohen, C.R., Crowley, N.J., Day, A.D., Donahue, M.N., Fry, L.J., Fuchs, H., Griffin, J.R., Guzman, I.M., Herrmann, H., Hodzic, A., Iinuma, Y., Jimenez, L.J., Kiendler-Scharr, A., Lee, H.B, Luecken, J.D., Mao, J., McLaren, R., Mutzel, A., Osthoff, D.H., Ouyang, B., Picquet-Varrault, B., Platt, U., Pye, T.O.H., Yinon Rudich, Y., Schwantes, H.R., Shiraiwa, M., Stutz, J., Thornton, A.J., Tilgner, A., Williams, J.B., Zaveri, A.R. Nitrate radicals and biogenic volatile organic compounds: oxidation, mechanisms, and organic aerosol. Atmos. Chem. Phys., 17, 2103–2162, https://doi.org/10.5194/acp-17-2103-2017, 2017.

Nuruzzaman, M. Urban heat island: Causes, effects and mitigation measures – A review. IJEMA, 3(2), 67–73, https://doi.org/10.11648/j.ijema.20150302.15, 2015.

Pan, S., Roy, A., Choi, Y., Eslami, E., Thomas, S., Jiang, X., Gao, O.H. Potential impacts of electric vehicles on air quality and health endpoints in the Greater Houston Area in 2040. Atmos. Environ. 207, 38–51, https://doi.org/10.1016/j.atmosenv.2019.03.022, 2019.

Poppe III, A.C., Burnett, T.R., Thun, J.M. Lung cancer, cardiopulmonary mortality, and long-term exposure to fine particulate air pollution. JAMA., 287(9), 1132–1141, https://doi.org/10.1001/jama.287.9.1132, 2002.

Requia, J.W., Mohamed, M., Higgins, D.C., Arain, A., Ferguson, M. How clean are electric vehicles? Evidence-based review of the effects of electric mobility on air polutants, greenhouse gas emissions and human health. Atmos. Environ., 185, 64–77, https://doi.org/10.1016/j.atmosenv.2018.04.040, 2018.

Rizvi, A.H.S., Agrawal, P., Batra, S., Nidhi, N., Singh, V. Assessing urban heat island intensity and emissions with compressed natural gas in non-commercial vehicles. Urb. Clim., 48, 101421, https://doi.org/10.1016/j.uclim.2023.101421, 2023.

Rosenfeld, H.A., Akbari, H., Romm, J. J., Pomeranz, M. Cool communities: strategies for heat island mitigation and smog reduction. Energy Build., 28(1), 51–62, https://doi.org/10.1016/S0378-7788(97)00063-7, 1998.

Schreyer, F., Luderer, G., Rodrigues, R., Pietzcker, R.C., Baumstark, L. Sugiyama, M., Brecha, R.J., Ueckerdt, F. Common but differentiated leadership: strategies and challenges for carbon neutrality by 2050 across industrialized economies. Environ. Res. Lett., 15(11), 114016, https://doi.org/10.1088/1748-9326/abb852, 2020.

https://doi.org/10.5194/egusphere-2024-1961
Preprint. Discussion started: 25 July 2024

Santiago, V.J., Inoue, K., Tonokura, K. Modeling ground ozone concentration changes after variations in precursor emissions and assessing teir beneits in the Kanto region of Japan. Atmosphere, 13(8), 1187, https://doi.org/10.3390/atmos13081187, 2022.

Sheehan, E.P., Bowman, M.F. Estimated effects of temperature on secondary organic aerosol concentrations. Environ. Sci. Technol., 35(11), 2129–2135, https://doi.org/10.1021/es001547g, 2001.

Shen, W., Han, W., Wallington, J.T., Winkler, L.S. China electricity generation greenhouse gas emission intensity in 2030: Implications for electric vehicles. Environ. Sci. Technol., 53(10), 6063–6072, https://doi.org/10.1021/acs.est.8b05264, 2019.

Shibata, Y., Morikawa, T. Review of the JCAP/JATOP air quality model study in Japan. Atmosphere, 12 (8), 943, https://doi.org/10.3390/atmos12080943, 2021.

Sillman, S. The use of NO_y, H_2O_2, and HNO_3 as indicators for ozone- NO_X-hydrocarbon sensitivity in urban locations. J. Geophys. Res., 100(D7), 14175–14188, https://doi.org/10.1029/94JD02953, 1995.

Sillman, S. The relation between ozone, NO_X and hydrocarbons in urban and polluted rural environments. Atmos. Environ., 33(12), 1821–1845, https://doi.org/10.1016/S1352-2310(98)00345-8, 1999.

Skamarock, W.C., Klemp, J.B., Dudhia,J., Gill, D.O., Barker, D.M. Duda, M.G., Huang, X.-Y., Wang, W., Powers, J.G. A description of the advanced research WRF version 4. NCAR Technical Note. http://pfigshare-u-files.s3.amazonaws.com/14057147/WRF_TechNote_Jan2019.pdf (accessed April 11, 2024).

Soet, A., Guevara, M., Baldasano, M.J. The potential impacts of electric vehicles on air quality in the urban areas of Barcelona and Madrid (Spain). Atmos. Environ., 99, 51–63, https://doi.org/10.1016/j.atmosenv.2014.09.048, 2014.

Stathopoulou, E., Mihalakakou, G., Santamouris, M., Bagiorgas, S. H. On the impact of temperature on tropospheric ozone concentration levels in urban environments. J. Earth Syst. Sci., 117, 227–236, https://doi.org/10.1007/s12040-008-0027-9, 2008.

Strapason, A., Woods, J., Pérez-Cirera, V., Elizondo, A., Cruz-Cano, D., Pestiaux, J., Cornet, M., Chaturvedi, R. Modelling carbon mitigation pathways by 2050: insights from the global calculator. Energy Strategy Rev., 29, 100494, https://doi.org/10.1016/j.esr.2020.100494, 2020.

Tonnesen, G.S., Dennis, R.L. Analysis of radical propagation efficiency to assess ozone sensitivity to hydrocarbons and NO_X: 2. Long-lived species as indicators of ozone concentration sensitivity. J. Geophys. Res., 105(D7), 9227–9241, https://doi.org/10.1029/1999JD900372, 2000.

Ulpiani, G. On the linkage between urban heat island and urban pollution island: Three-decade literature review towards a conceptual framework. Sci. Total Environ. 751, 141727, https://doi.org/10.1016/j.scitotenv.2020.141727, 2021.

Vander, A.R. Tropospheric emission monitoring internet service. https://www.temis.nl/index.php (Accessed May 21, 2024)

van Geffen, J., oersma, F.K., Eskes, H., Sneep, M., ter Linden, M., Zara, M., Veefkind, P.J. S5P TROPOMI NO2 slant column retrieval: method, stability, uncertainties and comparisons with OMI. Atmos. Meas. Tech., 13, 1315–1335, https://doi.org/10.5194/amt-13-1315-2020, 2020.

https://doi.org/10.5194/egusphere-2024-1961
Preprint. Discussion started: 25 July 2024

Vereecken, L., Novelli, A., Taraborrelli, D. Unimolecular decay strongly limits the atmospheric impact of Criegee intermediates. Phys. Chem. Chem. Phys., 19, 31599–31612, https://doi.org/10.1039/C7CP05541B, 2017.

Volkamer, R., Jimenez, L.J. Martini, S.F., Dzepina, K., Zhang, Q., Salcedo, D., Molina, T.L., Worsnop. R.D., Molina, J.M. Secondary organic aerosol formation from anthropogenic air pollution: Rapid and higher than expected. Geo. Phys. Lett., 33(17), L17811, https://doi.org/10.1029/2006GL026899, 2006.

Wang, Y., Du, H., Xu, Y., Lu, D., Wang, X., Guo, Z. Temporal and spatial variation relationship and influence factors on surface urban heat island and ozone pollution in the Yangtze River Delta, China. Sci. Total Environ., 631-632, 921–933, https://doi.org/10.1016/j.scitotenv.2018.03.050, 2018.

Warneke, C., de Gouw, A.J., Goldan, D.P., Kuster, C.W., Williams, J.E. Lerner, M.B., Jakoubek, R., Brown, S.S., Stark, H., Aldener, M., Ravishankara, A.R., Roberts, M.J., Marchewka, M., Bertman, S., Sueper, T.D., McKeen, A.S., Meagher, F.J., Fehsenfeld, C.F. Comparison of daytime and nighttime oxidation of biogenic and anthropogenic VOCs along the New England coast in summer during New England Air Quality Study 2002. J. Geophys. Res. Atmos., 109(D10), https://doi.org/10.1029/2003JD004424, 2004.

WHO Regional Office for Europe, Copenhagen. Health risks of ozone from long-range transboundary air pollution. 2008. ISBN: 9789289042895.

Xie, M., Zhu, K, Wang, T, Feng, W, Gao, D, Li, M, Li, S., Zhuang, B., Han, Y., Chen, P., Liao, J. Changes in regional meteorology induced by anthropogenic heat and their impacts on air quality in South China. Atmos. Chem. Phys., 16, 15011–15031, https://doi.org/10.5194/acp-16-15011-2016, 2016.

Yamada, H., Inomata, S., Tanimoto, H., Hata, H., Tonokura, K. Estimation of refueling emissions based on theoretical model and effects of E10 fuel on refueling and evaporative emissions from gasoline cars. Sci. Total Environ., 622–623, 467–473, https://doi.org/10.1016/j.scitotenv.2017.11.339, 2018.